

# UCLA

## UCLA Previously Published Works

### Title

Constraining crustal silica on ancient Earth

### Permalink

<https://escholarship.org/uc/item/8vp0490q>

### Journal

Proceedings of the National Academy of Sciences of the United States of America, 117(35)

### ISSN

0027-8424

### Authors

Keller, C Brenhin

Harrison, T Mark

### Publication Date

2020-09-01

### DOI

10.1073/pnas.2009431117

Peer reviewed



# Constraining crustal silica on ancient Earth

C. Brenhin Keller<sup>a,1</sup> and T. Mark Harrison<sup>b,1</sup>

<sup>a</sup>Department of Earth Sciences, Dartmouth College, Hanover, NH 03755; and <sup>b</sup>Department of Earth, Planetary, and Space Sciences, University of California, Los Angeles, CA 90095

Contributed by T. Mark Harrison, July 21, 2020 (sent for review May 15, 2020; reviewed by Francis Albarède and Jun Korenaga)

**Accurately quantifying the composition of continental crust on Hadean and Archean Earth is critical to our understanding of the physiography, tectonics, and climate of our planet at the dawn of life. One longstanding paradigm involves the growth of a relatively mafic planetary crust over the first 1 to 2 billion years of Earth history, implying a lack of modern plate tectonics and a paucity of subaerial crust, and consequently lacking an efficient mechanism to regulate climate. Others have proposed a more uniformitarian view in which Archean and Hadean continents were only slightly more mafic than at present. Apart from complications in assessing early crustal composition introduced by crustal preservation and sampling biases, effects such as the secular cooling of Earth's mantle and the biologically driven oxidation of Earth's atmosphere have not been fully investigated. We find that the former complicates efforts to infer crustal silica from compatible or incompatible element abundances, while the latter undermines estimates of crustal silica content inferred from terrigenous sediments. Accounting for these complications, we find that the data are most parsimoniously explained by a model with nearly constant crustal silica since at least the early Archean.**

continental crust | plate tectonics | Archean | Hadean

**A** lone among the planets of our solar system, Earth possesses two compositionally and morphologically distinct types of crust—a basaltic variety underlying the oceans, and a higher-silica type comprising the continents. Of these two, the oceanic crust is more analogous in composition to the crusts of other silicate planets, while the felsic continental crust is the anomaly (1–4). In this context, it has long been suggested that the existence of continental crust is due to a feedback system whereby subduction of ocean water to the mantle catalyzes the production of felsic magmas by altering solidus temperature, viscosity, and phase relationships during magmatic differentiation (3). In turn, those buoyant, felsic magmas stabilize liquid water at Earth's surface by forming subaerial crust whose weathering draws down atmospheric CO<sub>2</sub>, thus preventing runaway greenhouse loss of surface oceans (5, 6).

There is a hard limit to the maximum age of Earth's first felsic (henceforth continental) crust, since energetic planetary accretion culminating in formation of Moon prior to 4.51 Ga (7, 8) likely left, in its wake, a primordial magma ocean (9). Crystallization of that magma could not itself have directly produced a felsic crust, due to the reaction of the latter with olivine to produce pyroxene. In the absence of any consensus on the subsequent formation and growth of Earth's continental crust (10, 11), two competing conceptual end member models have emerged. In the first, what Moorbath (12) characterized as the “majority view” of continental crust growth, Earth features predominantly mafic crust, no plate tectonics, and (presumably) a less well-regulated climate until sometime in the mid-Archean (e.g., refs. 13–18). The second more uniformitarian view posits felsic continental crust (and thus subduction) and relatively equable climate since and possibly during the Hadean (10, 19–21). Consequently, the question of Earth's ancient crustal composition is deeply connected to our inference of the physiography, tectonics, and climate of our planet at the dawn of life.

Our ability to determine the past composition of the continental crust is, however, limited by the very same processes that

make our planet habitable: erosion by the wind, rain, and ice of an active hydrosphere; the slow return of ancient felsic crust to the mantle by sediment subduction and subduction–erosion; and the assimilation and metamorphism accompanying the birth of new crust from mantle-derived magma (e.g., ref. 22). In comparison to currently quiescent worlds like Mars (23) or our Moon (24), most of Earth's crust is geologically young (25). While this first-order challenge is well known, recent estimates of the composition of Earth's Archean crust have nonetheless reached widely divergent results, from mafic (15–18) to felsic (26–28).

We suggest that these divergent results may be explained by two factors that have been even less appreciated than the first-order biases introduced by incomplete sampling (29) and preferential preservation of weakly radioactive crust (30): 1) the secular cooling of Earth's mantle and 2) the radically changing oxidation state of Earth's atmosphere and hydrosphere, driven primarily by oxygenic photosynthesis.

Secular mantle cooling is widely expected as a consequence of Earth's ongoing loss of heat, today estimated to be about 46 terawatts (31), compounded by exponentially declining radiogenic heat production (31, 32). The primary observable consequence is the declining melt fraction in mantle magmas, as has long been noted in the context of the declining abundance of komatiites (magnesian magmas produced by high-degree melting of mantle peridotite) since the Archean (33, 34). This declining melt fraction results in changing major element systematics of mantle-derived basalts, notably including decreasing MgO (35, 36). The rather straightforward generalization of this phenomenon to compatible and incompatible trace elements is discussed at some length by Keller and Schoene (37, 38); in brief, compatible element concentrations decrease while incompatible element concentrations increase in preserved continental basalts over the past 4 Gyr.

## Significance

**On geologic timescales, Earth's habitable climate is maintained by a negative feedback process wherein atmospheric CO<sub>2</sub> is consumed by reaction with silicate rocks during erosion and weathering. However, relative to modern continental crust, many models propose an ancient crust that was thinner, denser, and significantly lower in silica for the first 1 to 2 billion years of Earth history. Like modern oceanic crust, such mafic crust would likely be poorly exposed to the atmosphere, resulting in a less climatically stable early Earth. We find that two geologic processes (mantle cooling and atmospheric oxidation) significantly compromise some previous methods for estimating ancient crustal composition. Accounting for these factors results in estimates much closer to the composition of modern continental crust.**

Author contributions: C.B.K. designed research; C.B.K. performed research; C.B.K. and T.M.H. analyzed data; and C.B.K. and T.M.H. wrote the paper.

Reviewers: F.A., University of Lyon System; and J.K., Yale University.

The authors declare no competing interest.

Published under the [PNAS license](#).

<sup>1</sup>To whom correspondence may be addressed. Email: cbkeller@dartmouth.edu or tmark.harrison@gmail.com.

First published August 17, 2020.

The second factor, the oxygenation of Earth's atmosphere and hydrosphere, is mediated primarily by biological factors: oxygenic photosynthesis. For much of Earth's early history, before 2,450 Ma, atmospheric oxygen is thought to have been less than  $10^{-5}$  of the modern partial pressure, as indicated by mass-independent sulfur isotope fractionation driven by atmospheric photochemical reactions that occur only in the absence of oxygen (39, 40). The path of subsequent oxygenation is less clear, but is thought to have reached comparatively modern, breathable levels by no later than 400 Ma (41–43). The effects of this oxygenation on the geochemistry and phase relations of exposed crust and sediment have been widely considered in other contexts (e.g., refs. 44 and 45), yet many estimates of Archean crustal composition rely critically on redox-sensitive trace element ratios in terrigenous sediments (e.g., refs. 16–18).

### Secular Variation as a Function of Silica Content

To further explore the difficulties posed by secular cooling for some previous estimates of Archean crustal composition, we employ the dataset and weighted bootstrap resampling approach of Keller and Schoene (37, 38). This weighted bootstrap resampling approach attempts to reduce sampling bias by assigning to each sample a resampling probability that is inversely related to spatiotemporal sample density (37, 38). However, more critical to the results than any improvement in evenness is simply the ability to accurately represent each measured value (be it age, silica,  $K_2O$ , etc.) as a distribution rather than as a single value. We accomplish this numerically, by adding Gaussian noise with appropriate variance to each sample in each resampling step—but an analogous result can be equally obtained by Gaussian kernel methods as in Ptáček et al. (28). As in Keller and Schoene (37, 38), the dataset includes data previously compiled by EarthChem (49) (including contributions from NAVDAT and GEOROC), Condie and O'Neill (50), and Moyen (51).

Since many studies rely upon trace element ratios as proxies to infer major element concentrations of the Archean crust (15–18), it is critical to understand the relationship between such ratios and  $SiO_2$  if we wish to infer Archean crustal silica content in this way. To quantify such relationships, and any potential variation therein over time, we calculate the mean (for single elements), median (for ratios), and 95% credible interval thereof for several elements and ratios binned as a function of  $SiO_2$ , for four age intervals: 0 Ga to 1 Ga, 1 Ga to 2 Ga, 2 Ga to 3 Ga, and 3 Ga to 4 Ga.

While perhaps less obvious than in sedimentary rocks, diagenetic and metasomatic processes, broadly defined, remain serious obstacles in the igneous record as well. Archean seafloor magmatic rocks, for instance, are commonly silicified, dramatically altering both major and trace element compositions (52). While we focus here on continental crust, not oceanic, we by no means warrant our calculations to be free of bias from metasomatic alteration and weathering. Rather, we aim to show that, even in the most benign scenario in which such effects are minimal, the use of trace element proxies to infer major element concentrations through time is fraught.

As seen in Fig. 1, the relationship between major and trace element concentrations with  $SiO_2$  has not been constant through time. For instance, MgO abundance has consistently decreased as a function of time at constant  $SiO_2$  (Fig. 1A), with the most significant changes occurring at low silica. Conversely,  $K_2O$  content has dramatically increased as a function of time for preserved continental igneous rocks of every  $SiO_2$  from basalt to granite (Fig. 1B). Similarly dramatic variations through time at constant silica are observed in a range of significant trace element ratios. In particular, as illustrated in Fig. 1C, Rb/Sr ratios were dramatically lower at a given  $SiO_2$  in the Archean, especially at the felsic end of the spectrum. Similarly large variations are

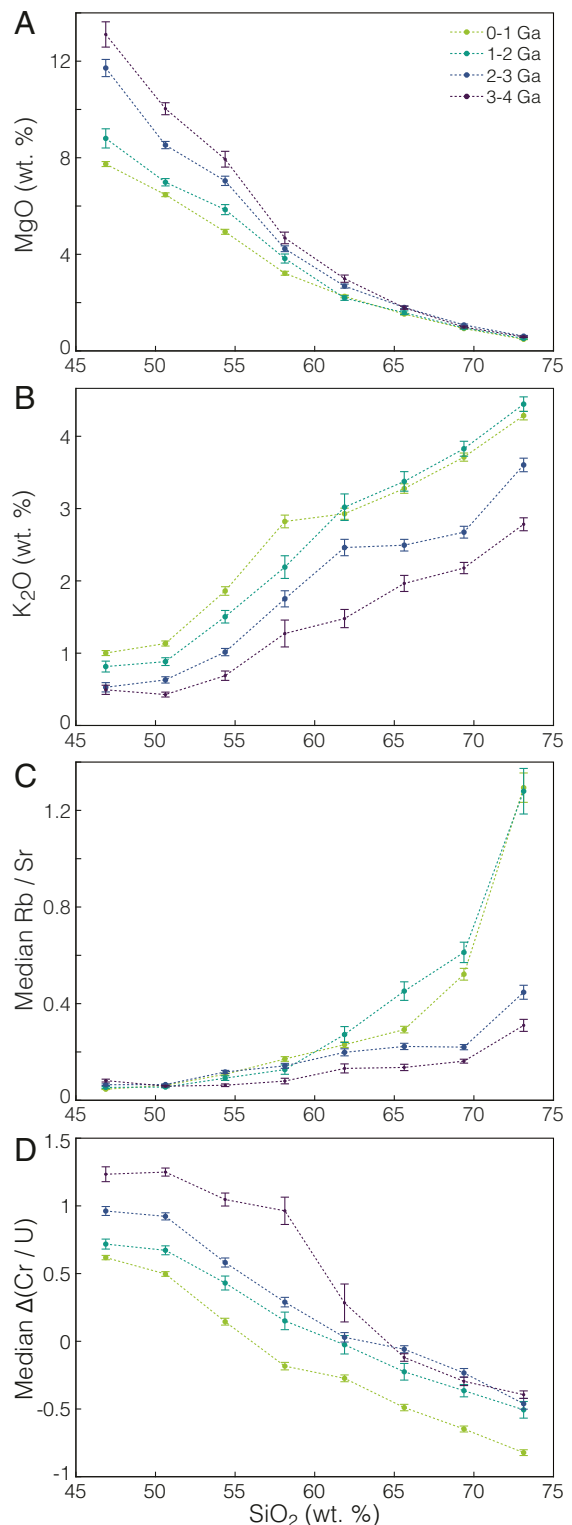


**Fig. 1.** Variations in MgO,  $K_2O$ , Rb/Sr, and Cr/U as a function of  $SiO_2$  for four gigayear-long time intervals between 0 Ga and 4 Ga, plotted as the mean (MgO and  $K_2O$ ) and median (Rb/Sr and Cr/U) along with the 95% credible interval thereof, determined using the dataset and weighted bootstrap resampling approach of Keller and Schoene (37, 38).

observed in Cr/U, this time with higher values in the Archean (Fig. 1D) as shown here in the  $\Delta$  (Cr/U) notation ( $\Delta$ (Cr/U) =  $\log(Cr/U) / \log(Cr/U)_{PAAS}$ , where PAAS is Post-Archean

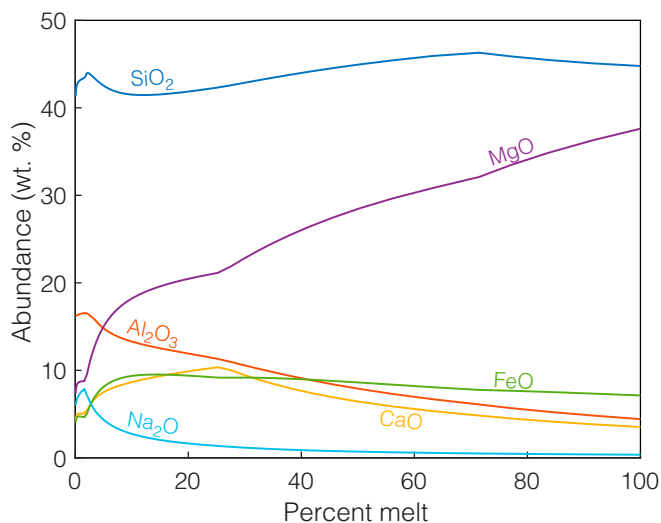


**Fig. 2.** Modeled melt composition, as a function of percent melt, that would result from mantle melting calculated using pMELTS-mode alphaMELTS simulations (46, 47) and the pyrolite composition of McDonough and Sun (48) at 2 GPa and 0.15 wt % H<sub>2</sub>O.

Australian Shale) of Smit and Mezger (17). Notably, such trends are not always monotonic as a function of time; on the contrary, while both broadly increase over time, K<sub>2</sub>O is slightly higher and Rb/Sr markedly higher for granodioritic and granitic compositions circa 2 Ga to 1 Ga than from 1 Ga to 0 Ga.

This result, varying compatible and incompatible element concentrations at constant silica, may seem counterintuitive if we approach the problem with an assumption that partial melting and fractional crystallization are diametrically opposed, that is, if we qualitatively consider higher-degree melts to be “more mafic” and lower-degree melts “more felsic.” In reality, such a description would be highly inaccurate. In contrast to calc-alkaline differentiation driven by hydrous fractional crystallization, which rapidly drives magmas to higher silica, the extent of mantle melting has remarkably little influence on magma SiO<sub>2</sub>. Instead, as illustrated in Fig. 2 for the case of isobaric equilibrium melting of McDonough and Sun (48) “pyrolite” primitive mantle at 2 GPa and 0.15 wt % H<sub>2</sub>O, magma SiO<sub>2</sub> fluctuates by only a few weight percent for melting extents between ~5% and 100%. That is to say, despite dramatic changes in mantle melting extent over time, the SiO<sub>2</sub> content of the resulting basalts—basalts which represent the primary mass flux from the mantle to the crust, and the starting point for crustal differentiation—has remained nearly constant.

If not accounted for, such effects significantly undermine the accuracy of trace element proxies for Archean crustal silica. To further illustrate this point, we consider, as a conceptual framework, a constant crustal silica reference model—or, more specifically, a reference model based on a null hypothesis that Archean crust featured the same relative proportions of mafic, felsic, and intermediate compositions as observed in the modern crust.

To produce the constant-silica model reference compositions shown herein, we first separate the observed compositions into three compositional bins: 43 to 55% SiO<sub>2</sub> (mafic), 55 to 65% SiO<sub>2</sub> (intermediate), and 65 to 78% (felsic). We then calculate the average value of each compositional variable of interest for each silica bin for each 100-Ma time interval between the present and 3,900 Ma. Finally, the constant-silica reference model average for each time bin is calculated by simply recombining (taking a weighted average) the average compositions for each silica bin

in proportion to their modern abundances, —44.9% from 43 to 55% SiO<sub>2</sub>, 23.4% from 55 to 65% SiO<sub>2</sub>, and 31.6% from 65 to 78% SiO<sub>2</sub>.

At present, the abundance of continental igneous rocks as a function of SiO<sub>2</sub> in many settings displays a pronounced bimodality sometimes referred to as the “Daly gap”—the larger-scale version of two phenomena with this name (53–56). Of these two compositional modes, the (mantle-derived) mafic mode includes a high proportion of extrusive basalts, while the felsic mode (produced by differentiation of the mafics) is dominated by intrusive granites, due to the well-known eruptibility contrast of mafic and felsic magmas in the context of hydrous stalling (56, 57). Consequently, this gap is frequently muted or absent in settings such as active arcs too young to have a well-exposed plutonic record, but is readily apparent in accreted arcs (58); otherwise, as shown by Keller (58), this marked compositional bimodality persists throughout the entirety of the preserved continental igneous record (Fig. 3).

Consequently, while there are slight variations in the positions of the two modes, and numerous temporal gaps potentially attributable to limited sampling, there is some reason to expect that the underlying process producing this bimodal distribution has been active throughout the preserved rock record. Indeed, at gigayear timescales, the proportions of mafic, felsic, and intermediate compositions observed in the preserved continental record in Fig. 3 are notably constant. As such, our constant silica reference model based on the null hypothesis of constant proportions, in fact, involves surprisingly little deviation from the observed proportions in each 1-Gyr time bin.

The results for a range of major and minor elements are shown in Fig. 4; the variations for each element in this figure may be considered the minimum level of change over time which must be exceeded in order to reject a null hypothesis of constant crustal silica. Such trends may be calculated for any element or ratio of interest using code available at [github.com/brenhinkeller/StatGeochem.jl](https://github.com/brenhinkeller/StatGeochem.jl). To first order, incompatible element concentrations increase through time while compatible element concentrations decrease through time even at constant silica as a direct effect of secular mantle cooling which, as we have shown, has relatively little impact on the silica content of mantle-derived magmas despite its well-established influence on major elements such as MgO, as well as compatible and incompatible trace elements (37, 38).

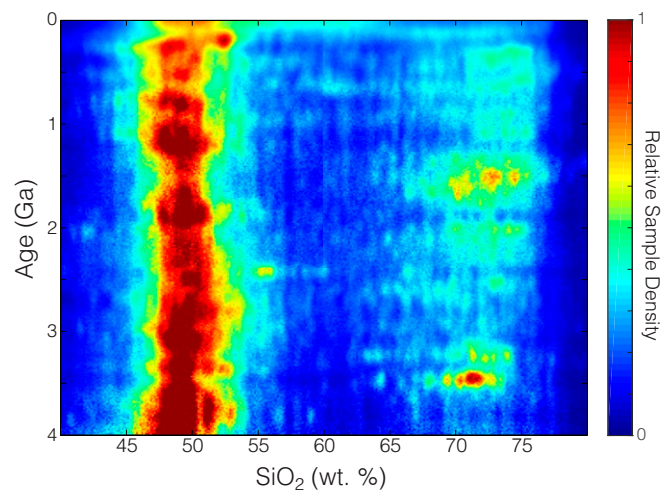


**Fig. 3.** Igneous whole-rock sample abundance as a function of age and SiO<sub>2</sub>, calculated and visualized as a two-dimensional histogram by C.B.K. (58) and reproduced here with permission; hotter colors represent greater sample abundance.

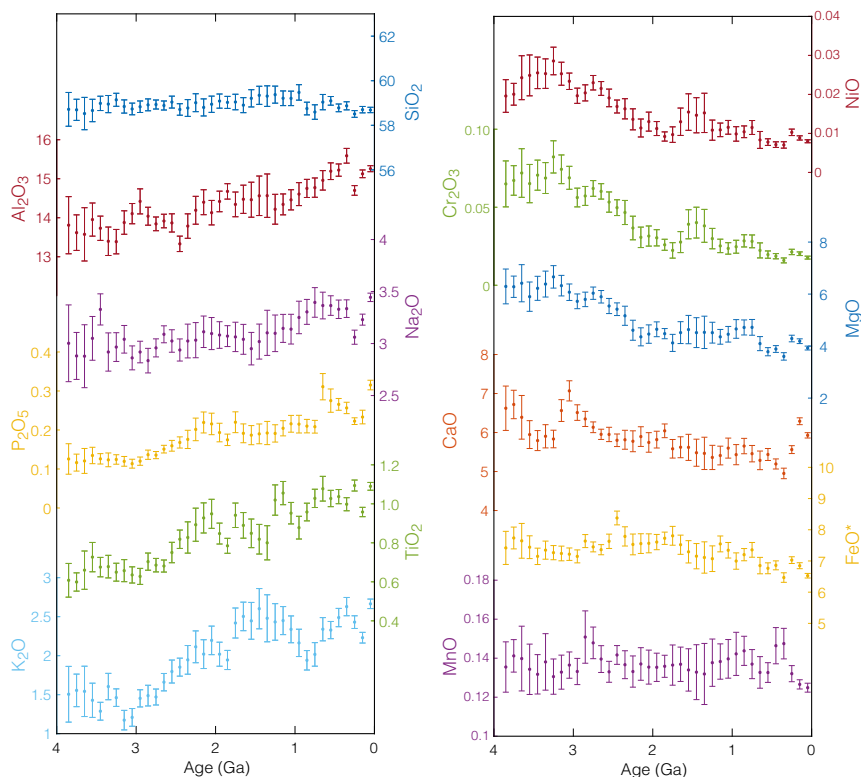


**Fig. 4.** Major and minor element concentrations for our constant-silica reference model, built to illustrate a null hypothesis that the proportion of mafic, intermediate, and felsic magmas has remained constant over time. Incompatible element concentrations increase through time while compatible element concentrations decrease through time even at constant silica as a first-order effect of secular mantle cooling which, as we have shown, has relatively little impact on the silica content of mantle-derived magmas despite its well-established influence on major elements such as MgO, as well as compatible and incompatible trace elements (37, 38).

For some trace element ratios, accounting for this variation in trace element abundances at constant silica causes previous models to entirely fail to reject the null hypothesis. For example, Dhuime et al. (15) use a compilation of  $^{87}\text{Sr}/^{86}\text{Sr}$  ratios, Rb/Sr ratios, Sm/Nd model ages, and crystallization ages for igneous rocks to infer the “juvenile” Rb/Sr ratio of an assumed protolith by calculating how much ingrowth of radiogenic  $^{87}\text{Sr}$  is required in the time between assumed extraction from the mantle (Sm/Nd model age) and crystallization of the observed sample to produce the observed Sr isotope ratio. They then use modern relationships between Rb/Sr ratio,  $\text{SiO}_2$ , and crustal thickness to argue that Earth’s continental crust transitioned from thin and mafic to thick and felsic starting around  $\sim 3$  Ga. However, as seen in Fig. 1C, the relationship between Rb/Sr and silica has been far from constant over time. In Fig. 5, we compare the estimated “juvenile” Rb/Sr ratios of Dhuime et al. (15) with our estimate of crustal Rb/Sr ratio in the null hypothesis case of constant crustal silica. While the model age-dependent method of Dhuime et al. (15) infers “juvenile” Rb/Sr ratios roughly a quarter of that observed in average crust, the trend matches our null hypothesis reference model within uncertainty, indicating that their variations in Rb/Sr over time can be explained solely by changing Rb/Sr at constant silica over time. While this temporal covariance is unlikely to result from secondary alteration [which would instead introduce anticovariance between our direct average and the isotopic approach of Dhuime et al. (15)], we emphasize that independent (e.g., isotopic) evidence supporting a lack of aqueous alteration would be required to ensure primary trace element preservation in large geochemical datasets, especially for highly fluid mobile element such as Rb and Sr.

Intriguingly, while the overall trend is to increasing Rb/Sr over time (consistent with the generally greater incompatibility of Rb), both records show declining average Rb/Sr ratio over the

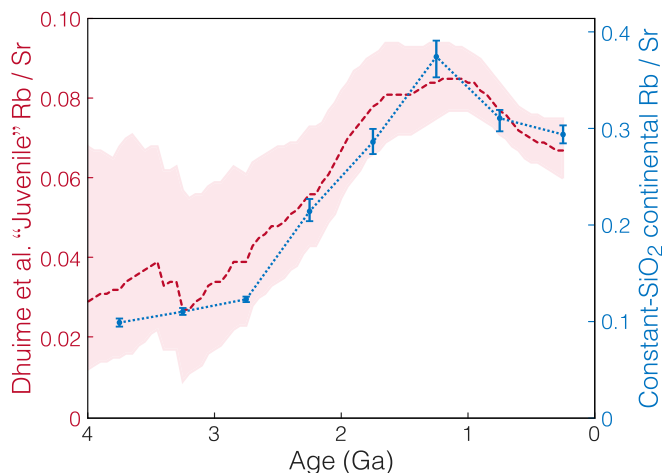


**Fig. 5.** Estimated “juvenile” Rb/Sr ratios of Dhuime et al. (15) (left axis) compared to our estimate of crustal Rb/Sr for a “constant-silica” crust (right axis) whose proportions of mafic, intermediate, and felsic rocks match those observed at present. While the model age-dependent method of Dhuime et al. (15) results in extremely low “juvenile” Rb/Sr ratios (roughly a quarter of that observed in average crust), the trend observed by Dhuime et al. (15) matches ours, indicating that the level of increase in Rb/Sr over time can be explained solely by secular cooling without any change in crustal  $\text{SiO}_2$ .



last  $\sim 1$  Gyr after reaching zenith *ca.* 1.4 Ga, despite ongoing secular cooling. We suggest that this peak may be associated with the remarkable high-K, high-Rb “A-type” granitoid event circa 1.4 Ga, first noted by Anderson and Bender (59). The degree to which this reflects a true global signal rather than a North American bias is less clear, but it is nonetheless remarkable how reproducible this phenomenon is across two greatly contrasting methodologies—both our direct whole-rock estimate and the isotopic approach of Dhuime et al. (15).

In other cases, such as the variations in Cr/U inferred from terrigenous sediment compositions by Smit and Mezger (17), secular variation in the relationship between the trace element proxy and silica only acts to reduce the magnitude—but not entirely eliminate—inferred changes in SiO<sub>2</sub>. For instance, as seen in Fig. 6A, the decrease in median igneous  $\Delta$  (Cr/U) for the constant-silica reference model appears to underestimate the decrease in  $\Delta$  (Cr/U) that would be inferred if the shale compositions of Smit and Mezger (17) are assumed to accurately reflect those of their igneous and metamorphic protoliths. Similarly, as seen in Fig. 6B, the MgO estimated from our constant-silica reference model broadly agrees with the estimate of Greber et al. (26), but significantly diverges from that of Tang et al. (16).

Finally, we may note that some other isotopic approaches, such as the titanium isotope method of Greber et al. (26), should be comparatively less sensitive to complications introduced by secular mantle cooling and its associated variations in mantle melting extent. A second-order complication might be introduced in this case if secular cooling resulted in a change in the ratio of plume to arc magmas incorporated into con-

tinental crust over time (60). However, such secular variation in the ratio of flux to decompression melting appears to be strongly excluded in basalts preserved in the continental crust from at least 3.8 Ga to the present (38) which reflect a consistent dominance of calc-alkaline differentiation over the entire interval.

### Atmospheric Oxygenation and Trace Element Ratios in Terrigenous Sediments

In an attempt to avoid preservation bias, many estimates of the composition of the Archean crust are based on the composition of terrigenous sediments, rather than directly upon the concentration of Archean igneous rocks (16–18, 26–28). While such an approach has advantages, it also brings risks. Many elements, especially those with low ionic charge-to-size ratios in their favored oxidation states, are soluble or partially soluble in aqueous fluids. This includes such elements as Ni and Co, used to estimate crustal silica by, for example, Tang et al. (16). Inauspiciously, the solubility of such fluid-mobile elements frequently varies as a function of redox state and/or pH, raising the specter of selective fractionation.

Such concerns are especially relevant given that proposed transitions in crustal silica (e.g., refs. 16–18) frequently coincide with the Great Oxidation Event (GOE), when Earth’s atmosphere first became significantly oxygenated. While perhaps best placed at 2,450 Ma on the basis of mass-independent sulfur isotope fractionation (39, 40), the process of gradual oxidation may have spanned a considerable interval, with debated “whiffs” proposed as early as 3 Ga (63), and a hypothesized “overshoot” as late as 2 Ga (64). However, the impacts of this transition on the use of trace element proxies in terrigenous sediments has been considered only perfunctorily, if at all, in previous studies (16–18). To illustrate the extent of this problem, we show, in Fig. 7, a range of Eh–pH (Pourbaix) diagrams (61) for several element pairs that have been previously employed to estimate crustal silica. Herein, we observe that, even considering only the system O–H–x, relevant minor and trace elements display marked variation in solubility at different Eh–pH conditions within the modern natural aqueous range (62)—soluble at some conditions but unavoidably precipitating as oxides or native metals at others.

For instance, while Smit and Mezger (17) acknowledge that Cr and U are redox-sensitive elements, they imply that this is a matter of only limited concern since both Cr and U are immobile when reduced, and thus “fractionation of Cr/U may be expected only in cases where Cr and U are not equally oxidized.” However, as seen in Fig. 7A, the stability limits of the insoluble oxidized forms of U (UO<sub>2</sub>; uraninite) and Cr (Cr<sub>2</sub>O<sub>3</sub>, in the system O–H–Cr) are markedly distinct, with Cr remaining insoluble at substantially higher Eh; this difference would be only exacerbated in a natural system with Fe to stabilize the Fe–Cr oxide mineral chromite. In the Archean, where detrital uraninite (along with pyrite) is commonly used as an indicator of low atmospheric pO<sub>2</sub> (65, 66), one might argue that, both U and Cr being relatively fluid immobile, shale Cr/U ratios could conceivably represent the protolith from which they were eroded. After the GOE, however, no such interpretation of sedimentary  $\Delta$  Cr/U is supportable. In addition to numerous other processes biasing the sedimentary record of redox-sensitive elements such as Cr and U (e.g., ref. 67), there appears to be, even in the most optimistic scenario, a transitional period (roughly spanning from the GOE to the Early Phanerozoic) in which detrital chromite is still widespread (e.g., refs. 68 and 69), but detrital uraninite is absent (65, 66), markedly decoupling Cr and U in sedimentary environments.

Equivalent difficulties apply to other sedimentary trace element proxies for crustal silica, including the Cr/Zn ratio of Tang

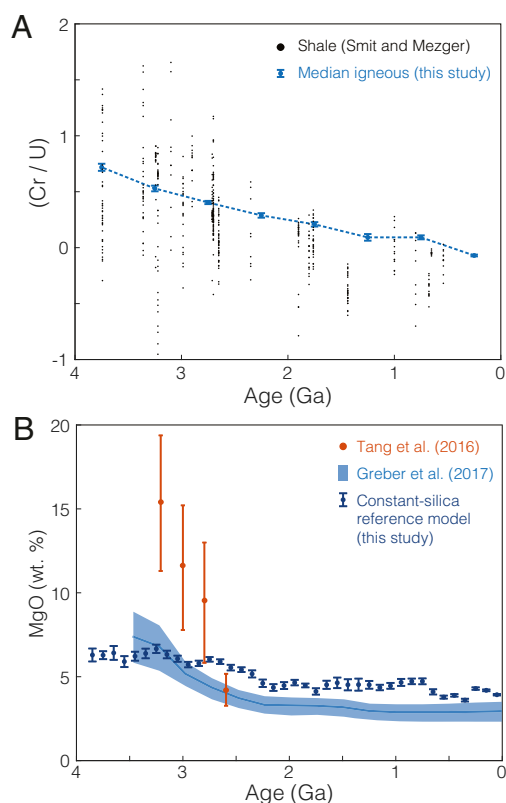


**Fig. 6.** (A) Variation in  $\Delta$  (Cr/U) over time as calculated for our constant-silica reference model, compared to the shale data of Smit and Mezger (17). The quantity  $\Delta$  (Cr/U) is defined by Smit and Mezger as  $\log(\text{Cr/U})/\log(\text{Cr/U})_{\text{PAA5}}$ . (B) The MgO content of our constant-silica reference model alongside the estimates of Greber et al. (26) and Tang et al. (16).

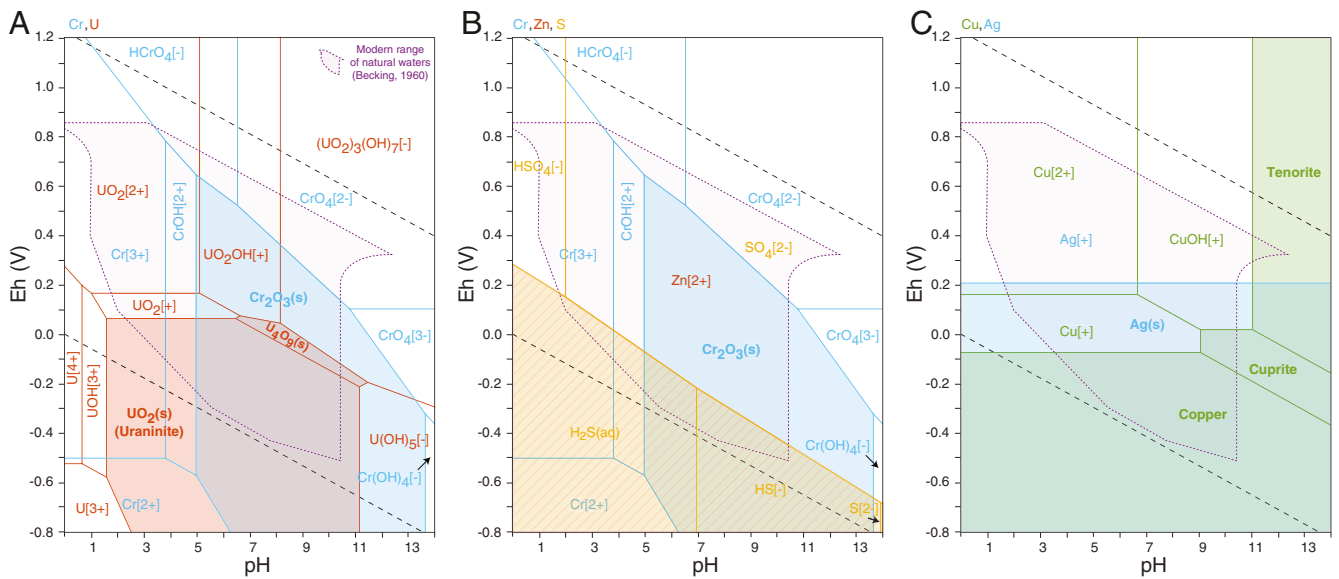


**Fig. 7.** Eh–pH (Pourbaix) diagrams for a range of trace and minor element pairs [(A) U and Cr; (B) S and Cr; (C) Cu and Ag], based on Lawrence Livermore National Laboratory dataset 3245r46, as computed by Takeno (61) for a solute concentration of  $10^{-10}$  M at 298.15 K and  $10^5$  Pa. The natural Eh–pH range of modern near-surface waters from Becking et al. (62) is shown for context; the upper limit thereof would be markedly reduced for Archean surface water and groundwater due to lower atmospheric  $pO_2$ . The stability limits of insoluble phases (bold) are shaded. In B, while Zn alone is soluble at all Eh–pH conditions, we additionally shade the stability range of sulfide, which, if cooccurring with certain otherwise soluble metals such as  $Zn^{2+}$ , would allow the formation of insoluble precipitates such as (in this case) sphalerite. Illustrated element pairs are especially subject to aqueous fractionation under any conditions where one is soluble and the other is not.

et al. (16) (Fig. 7B) and the Cu/Ag ratio of Chen et al. (18) (Fig. 7C), both of which are liable to fractionate due to weathering at different Eh–pH conditions. The situation becomes only more concerning when a fuller range of elements is considered beyond the O–H–x system. For instance, while Zn alone is soluble at all Eh–pH conditions, its solubility in natural low-Eh conditions would depend heavily on the availability of sulfide, which, if present, would allow the formation of insoluble metal sulfide precipitates (in this case, sphalerite). A similarly trivial attempt to quantify the redox dependence of an element ratio such as Ni/Co would require us to evaluate, at a minimum, the relative stability ranges of Ni and Co sulfides and sulfosalts; a more robust analysis would include the sorption of Ni and Co to other mineral surfaces (especially of clays) (e.g., refs. 70 and 71), the mineralogy of which may, in turn, change as a function of  $O_2$ . Indeed, the Ni/Co ratio of soils has been observed to strongly covary with proxies for the extent of oxidative weathering, such as  $Ce/Ce^*$  (72). Such effects appear to present a parsimonious explanation for the extraordinarily rapid rate of change inferred from such ratios by Tang et al. (16) across the GOE, and the contrast thereof with the relatively gradual decrease suggested by Greber et al. (26) and our reference model.

In brief, the use of potentially fluid-mobile trace element ratios in terrigenous sediment to infer crustal silica should be strongly resisted. Full mass balance models that include a wide range of elements with different redox sensitivities appear to be more robust to such effects (e.g., refs. 27 and 28), especially if care is taken to avoid contamination of the sedimentary signal by alteration and diagenesis (e.g., ref. 28). Extreme caution is nonetheless advised in any attempt to infer the composition of primary igneous crust that involves potentially fluid-mobile trace or minor elements in clastic detritus.

## Conclusions

The geochemical community has long favored a view that early terrestrial crust was broadly mafic, in part owing to misconceptions regarding both feldspar buoyancy on a hydrous magmatic

substrate and the deep stabilization of restitic garnet which retards crystallization of aluminous phases from derived melts (13–15) (cf. refs. 24 and 73). It follows from this conceptual framework that the simplest evolution to the present felsic crust occurred either in a monotonic fashion or during a discontinuity related to the discrete onset of subduction (e.g., ref. 15).

The composition of the continental crust has clearly changed over Earth history. For example, there is evidence for a progressive depletion in compatible elements (e.g., Cr) and enrichment in incompatible elements (e.g., Rb). However, the early Earth mantle was almost certainly hotter than today, resulting in higher degrees of mantle partial melting; as a result, incompatible element abundances were almost certainly lower than today (37, 38). By not taking this effect into account, we show, using a reference model characterized by constant proportions of mafic, intermediate, and felsic rocks (i.e., constant  $SiO_2$ ), that incorrect inferences regarding secular changes to the composition of continental crust (15) can result. Further errors are introduced when fluid-mobile and redox-sensitive trace element ratios in terrigenous sediments are used to indirectly estimate the composition of the continental crust (e.g., refs. 16–18). Notably, our analysis of a constant-silica reference model leads to conclusions similar to several other recent reevaluations (26–28). This observation, especially in the context of recent results suggesting a consistent dominance of arc-style flux melting throughout the preserved rock record (38), presents a challenge to the long-standing paradigm of early mafic crust, warranting further examination.

**Data Availability.** All underlying data and computational source code are available at GitHub, [github.com/brenhinkeller/StatGeochem.jl](https://github.com/brenhinkeller/StatGeochem.jl). All study data are included in the article and *SI Appendix*.

**ACKNOWLEDGMENTS.** Many of the concepts herein were originally developed over the course of discussion and collaboration with Patrick Boehnke, who declined to participate as an author of the present manuscript after transitioning to the private sector. T.M.H. is supported through a grant from the NSF Instrumentation and Facilities Program.

1. G. N. Katterfel'd, K. Benesh, V. Y. Khain, Y. A. Khodak, Problems of comparative planetology. *Int. Geol. Rev.* **10**, 989–1017 (1968).
2. P. D. Lowman Jr, "Evolution of the earth's crust: Evidence from comparative planetology" (Tech. Rep. TM-X-70539, NASA, 1973).
3. I. H. Campbell, S. R. Taylor, No water, no granites—No oceans, no continents. *Geophys. Res. Lett.* **10**, 1061–1064 (1983).
4. S. R. Taylor, Growth of planetary crusts. *Tectonophysics* **161**, 147–156 (1989).
5. J. C. G. Walker, P. B. Hays, J. F. Kasting, A negative feedback mechanism for the long-term stabilization of Earth's surface temperature. *J. Geophys. Res.* **86**, 9776–9782 (1981).
6. K. Caldeira, Long-term control of atmospheric carbon dioxide; low-temperature seafloor alteration or terrestrial silicate-rock weathering? *Am. J. Sci.* **295**, 1077–1114 (1995).
7. M. Barboni *et al.*, Early formation of the Moon 4.51 billion years ago. *Sci. Adv.* **3**, e1602365 (2017).
8. M. M. Thiemens, P. Sprung, R. O. C. Fonseca, F. P. Leitzke, C. Münker, Early Moon formation inferred from hafnium–tungsten systematics. *Nat. Geosci.* **12**, 696–700 (2019).
9. P. H. Warren, The magma ocean concept and lunar evolution. *Annu. Rev. Earth Planet. Sci.* **13**, 201–240 (1985).
10. T. M. Harrison, The Hadean crust: Evidence from 4 Ga zircons. *Annu. Rev. Earth Planet. Sci.* **37**, 479–505 (2009).
11. J. Korenaga, Initiation and evolution of plate tectonics on Earth: Theories and observations. *Annu. Rev. Earth Planet. Sci.* **41**, 117–151 (2013).
12. S. Moorbath, Precambrian geology: The most ancient rocks? *Nature* **304**, 585–586 (1983).
13. K. C. Condie, Plate-tectonics model for Proterozoic continental accretion in the southwestern United States. *Geology* **10**, 37–42 (1982).
14. S. R. Taylor, Lunar and terrestrial crusts—A contrast in origin and evolution. *Phys. Earth Planet. Inter.* **29**, 233–241 (1982).
15. B. Dhume, A. Wuestefeld, C. J. Hawkesworth, Emergence of modern continental crust about 3 billion years ago. *Nat. Geosci.* **8**, 552–555 (2015).
16. M. Tang, K. Chen, R. L. Rudnick, Archean upper crust transition from mafic to felsic marks the onset of plate tectonics. *Science* **351**, 372–375 (2016).
17. M. A. Smit, K. Mezger, Earth's early O<sub>2</sub> cycle suppressed by primitive continents. *Nat. Geosci.* **10**, 788–792 (2017).
18. K. Chen *et al.*, How mafic was the Archean upper continental crust? Insights from Cu and Ag in ancient glacial diamictites. *Geochem. Cosmochim. Acta* **278**, 16–29 (2019).
19. R. L. Armstrong, R. S. Harmon, Radiogenic isotopes: The case for crustal recycling on a near-steady-state no-continental-growth earth. *Philos. Trans. R. Soc. Lond. A* **301**, 443–472 (1981).
20. J. C. Rosas, J. Korenaga, Rapid crustal growth and efficient crustal recycling in the early earth: Implications for Hadean and Archean geodynamics. *Earth Planet. Sci. Lett.* **494**, 42–49 (2018).
21. M. Guo, J. Korenaga, Argon constraints on the early growth of felsic continental crust. *Sci. Adv.* **6**, eaaz6234 (2020).
22. J. Korenaga, Crustal evolution and mantle dynamics through Earth history. *Philos. Trans. R. Soc. A Math. Phys. Eng. Sci.* **376**, 20170408 (2018).
23. K. A. Farley *et al.*, In situ radiometric and exposure age dating of the martian surface. *Science* **343**, 1247166 (2014).
24. P. H. Warren, Growth of the continental crust: A planetary-mantle perspective. *Tectonophysics* **161**, 165–199 (1989).
25. P. M. Hurley, J. R. Rand, Pre-drift continental nuclei. *Science* **164**, 1229–1242 (1969).
26. N. D. Greber *et al.*, Titanium isotopic evidence for felsic crust and plate tectonics 3.5 billion years ago. *Science* **357**, 1271–1274 (2017).
27. N. D. Greber, N. Dauphas, The chemistry of fine-grained terrigenous sediments reveals a chemically evolved Paleoproterozoic emerged crust. *Geochem. Cosmochim. Acta* **255**, 247–264 (2019).
28. M. P. Ptáček, N. Dauphas, N. D. Greber, Chemical evolution of the continental crust from a data-driven inversion of terrigenous sediment compositions. *Earth Planet. Sci. Lett.* **539**, 116090 (2020).
29. T. M. Harrison, E. A. Bell, P. Boehnke, Hadean zircon petrochronology. *Rev. Mineral. Geochem.* **83**, 329–363 (2017).
30. P. Morgan, Crustal radiogenic heat production and the selective survival of ancient continental crust. *J. Geophys. Res.* **90**, C561–C570 (1985).
31. C. Jaupart, S. Labrosse, J. C. Mareschal, "Temperatures, heat and energy in the mantle of the Earth" in *Treatise on Geophysics*, G. Schubert, Ed. (Elsevier, 2007), pp. 253–303.
32. J. Korenaga, Energetics of mantle convection and the fate of fossil heat. *Geophys. Res. Lett.* **30**, 1437 (2003).
33. M. J. Viljoen, R. P. Viljoen, The geology and geochemistry of the lower ultramafic unit of the overvacht group and a proposed new class of igneous rock. *Geol. Soc. S. Afr. Spec. Publ.* **2**, 221–244 (1969).
34. D. H. Green, Genesis of archaean peridotitic magmas and constraints on Archean geothermal gradients and tectonics. *Geology* **3**, 15–18 (1975).
35. K. C. Condie, Chemical composition and evolution of the upper continental crust: Contrasting results from surface samples and shales. *Chem. Geol.* **104**, 1–37 (1993).
36. C. Herzberg, K. C. Condie, J. Korenaga, Thermal history of the Earth and its petrological expression. *Earth Planet. Sci. Lett.* **292**, 79–88 (2010).
37. C. B. Keller, B. Schoene, Statistical geochemistry reveals disruption in secular lithospheric evolution about 2.5 Gyr ago. *Nature* **485**, 490–493 (2012).
38. C. B. Keller, B. Schoene, Plate tectonics and continental basaltic geochemistry throughout Earth history. *Earth Planet. Sci. Lett.* **481**, 290–304 (2018).
39. J. Farquhar, H. Bao, M. Thiemens, Atmospheric influence of Earth's earliest sulfur cycle. *Science* **289**, 756–758 (2000).
40. A. P. Gumsley *et al.*, Timing and tempo of the Great Oxidation Event. *Proc. Natl. Acad. Sci. U.S.A.* **114**, 1811–1816 (2017).
41. A. C. Scott, I. J. Glasspool, The diversification of paleozoic fire systems and fluctuations in atmospheric oxygen concentration. *Proc. Natl. Acad. Sci. U.S.A.* **103**, 10861–10865 (2006).
42. E. A. Sperling *et al.*, Statistical analysis of iron geochemical data suggests limited late Proterozoic oxygenation. *Nature* **523**, 451–454 (2015).
43. D. A. Stolper, C. B. Keller, A record of deep-ocean dissolved O<sub>2</sub> from the oxidation state of iron in submarine basalts. *Nature* **553**, 323–327 (2018).
44. H. D. Holland, N. J. Beukes, A paleoweathering profile from Griqualand West, South Africa: Evidence for a dramatic rise in atmospheric oxygen between 2.2 and 1.9 bybp. *Am. J. Sci.* **290-A**, 1–34 (1990).
45. R. M. Hazen *et al.*, Mineral evolution. *Am. Mineral.* **93**, 1693–1720 (2008).
46. M. S. Ghiorso, M. M. Hirschmann, P. W. Reiners, V. C. Kress, III, The pMELTS: A revision of MELTS for improved calculation of phase relations and major element partitioning related to partial melting of the mantle to 3 GPa. *Geochem. Geophys. Geosyst.* **3**, 1–36 (2002).
47. P. M. Smith, P. D. Asimow, Adiabatic 1ph: A new public front-end to the MELTS, pMELTS, and pHMELTS models. *Geochem. Geophys. Geosyst.* **6**, 1–8 (2005).
48. W. F. McDonough, S. S. Sun, The composition of the Earth. *Chem. Geol.* **120**, 223–253 (1995).
49. EarthChem, EarthChem Portal (2010). <http://www.earthchem.org/portal>. Accessed 14 February 2011.
50. K. C. Condie, C. O'Neill, The Archean-Proterozoic boundary: 500 my of tectonic transition in Earth history. *Am. J. Sci.* **310**, 775–790 (2010).
51. J. F. Moyen, The composite Archean grey gneisses: Petrological significance, and evidence for a non-unique tectonic setting for Archean crustal growth. *Lithos* **123**, 21–36 (2010).
52. L. André *et al.*, Early continental crust generated by reworking of basalts variably silicified by seawater. *Nat. Geosci.* **12**, 769–773 (2019).
53. R. A. Daly, The geology of Ascension Island. *Proc. Am. Acad. Arts Sci.* **60**, 3–80 (1925).
54. O. Reubi, J. D. Blundy, A dearth of intermediate melts at subduction zone volcanoes and the petrogenesis of arc andesites. *Nature* **461**, 1269–1273 (2009).
55. J. Dufek, O. Bachmann, Quantum magmatism: Magmatic compositional gaps generated by melt-crystal dynamics. *Geology* **38**, 687–690 (2010).
56. C. B. Keller, B. Schoene, M. Barboni, K. M. Samperton, J. M. Husson, Volcanic–plutonic parity and the differentiation of the continental crust. *Nature* **523**, 301–307 (2015).
57. H. G. F. Winkler, Viel Basalt und wenig Gabbro–Wenig Rhyolith und viel Granit. *Beitr. Mineral. Petrogr.* **8**, 222–231 (1962).
58. C. B. Keller, "Geochemical evolution of Earth's continental crust," PhD thesis, Princeton University, Princeton, NJ (2016).
59. J. L. Anderson, E. E. Bender, Nature and origin of proterozoic A-type granitic magmatism in the southwestern United States of America. *Lithos* **23**, 19–52 (1989).
60. Z. Deng *et al.*, Titanium isotopes as a tracer for the plume or island arc affinity of felsic rocks. *Proc. Natl. Acad. Sci. U.S.A.* **116**, 1132–1135 (2019).
61. N. Takeda, "Atlas of eh-pH diagrams" (Open File Rep. 419, Geological Survey of Japan, 2005).
62. L. G. M. B. Becking, I. R. Kaplan, D. Moore, Limits of the natural environment in terms of pH and oxidation-reduction potentials. *J. Geol.* **68**, 243–284 (1960).
63. S. A. Crowe *et al.*, Atmospheric oxygenation three billion years ago. *Nature* **501**, 535–538 (2013).
64. K. S. Rybacki, L. R. Kump, E. J. Hanski, V. A. Melezhik, Weathering during the great oxidation event: Fennoscandia, arctic Russia 2.06 Ga ago. *Precambrian Res.* **275**, 513–525 (2016).
65. B. Rasmussen, R. Buick, Redox state of the Archean atmosphere: Evidence from detrital heavy minerals in ca. 3250–2750 Ma sandstones from the Pilbara Craton, Australia. *Geology* **27**, 115–118 (1999).
66. J. E. Johnson, A. Gerpheide, M. P. Lamb, W. W. Fischer, O<sub>2</sub> constraints from Paleoproterozoic detrital pyrite and uraninite. *Geol. Soc. Am. Bull.* **126**, 813–830 (2014).
67. C. A. Partin *et al.*, Large-scale fluctuations in Precambrian atmospheric and oceanic oxygen levels from the record of U in shales. *Earth Planet. Sci. Lett.* **369–370**, 284–293 (2013).
68. U. Giese, R. Walter, G. Katzung, Detrital composition of Ordovician sandstones from the Rügen boreholes: Implications for the evolution of the Tornquist Ocean. *Geol. Rundsch.* **83**, 293–308 (1994).
69. J. I. Garver, P. R. Royce, T. A. Smick, Chromium and nickel in shale of the tectonic foreland: A case study for the provenance of fine-grained sediments with an ultramafic source. *J. Sediment. Res.* **66**, 100–106 (1996).
70. M. Elias, M. J. Donaldson, N. E. Giorgetta, Geology, mineralogy, and chemistry of lateritic nickel-cobalt deposits near Kalgoorlie, Western Australia. *Econ. Geol.* **76**, 1775–1783 (1981).
71. A. Gaudin, A. Decarreau, Y. Noack, O. Grauby, Clay mineralogy of the nickel laterite ore developed from serpentinized peridotites at Murrin Murrin, Western Australia. *Aust. J. Earth Sci.* **52**, 231–241 (2005).
72. A. T. Gourlan, F. Albarède, H. Achyuthan, S. Campillo, The marine record of the onset of farming around the Arabian Sea at the dawn of the Bronze Age. *The Holocene* **30**, 878–887 (2020).
73. H. Zou, T. M. Harrison, Formation of 4.5 Ga continental crust. *Geochem. Cosmochim. Acta* **71**, A1176 (2007).